

RESEARCH OUTPUTS / RÉSULTATS DE RECHERCHE

Aluminum pretreatment by a laser ablation process

Al Sayyad, Adham; Bardon, Julien; Hirchenhahn, Pierre; Santos, Kevin; Houssiau, Laurent; Plapper, Peter

Published in:
Procedia CIRP

DOI:
[10.1016/j.procir.2018.08.136](https://doi.org/10.1016/j.procir.2018.08.136)

Publication date:
2018

Document Version
Publisher's PDF, also known as Version of record

[Link to publication](#)

Citation for published version (HARVARD):

Al Sayyad, A, Bardon, J, Hirchenhahn, P, Santos, K, Houssiau, L & Plapper, P 2018, Aluminum pretreatment by a laser ablation process: influence of processing parameters on the joint strength of laser welded aluminum - Polyamide assemblies. in M Schmidt, F Vollertsen & G Dearden (eds), *Procedia CIRP: 10th CIRP Conference on Photonic Technologies [LANE 2018]*. Procedia CIRP, vol. 74, pp. 495-499, 10th CIRP Conference on Photonic Technologies, LANE 2018, Furth, Germany, 3/09/18. <https://doi.org/10.1016/j.procir.2018.08.136>

General rights

Copyright and moral rights for the publications made accessible in the public portal are retained by the authors and/or other copyright owners and it is a condition of accessing publications that users recognise and abide by the legal requirements associated with these rights.

- Users may download and print one copy of any publication from the public portal for the purpose of private study or research.
- You may not further distribute the material or use it for any profit-making activity or commercial gain
- You may freely distribute the URL identifying the publication in the public portal ?

Take down policy

If you believe that this document breaches copyright please contact us providing details, and we will remove access to the work immediately and investigate your claim.

10th CIRP Conference on Photonic Technologies [LANE 2018]

Aluminum Pretreatment by a Laser Ablation Process: Influence of Processing Parameters on the Joint Strength of Laser Welded Aluminum – Polyamide Assemblies

Adham Al-Sayyad^{a,*}, Julien Bardon^b, Pierre Hirchenhahn^c, Kevin Santos^a, Laurent Houssiau^c,
Peter Plapper^a

^aUniversity of Luxembourg, rue Coudenhove-Kalergi 6, L-1359 Luxembourg, Luxembourg

^bLuxembourg Institute of Science and Technology, avenue des Hauts-Fourneaux 5, L-4362 Esch-sur-Alzette, Luxembourg

^cUniversité de Namur, NISM Namur Institute for Structured Matter, LISE, Rue de Bruxelles 61, 5000 NAMUR, Belgium

* Corresponding author. Tel.: +352-466644-6034; fax: +352-466644-36034. E-mail address: adham.alsayyad@uni.lu

Abstract

Laser welding of metal – polymer assemblies is an innovative bonding process. It was already demonstrated that laser surface pretreatments of aluminum (Al), prior to laser welding with a polymer, impacts joints strength. This work adopts a design of experiments (DoE) approach to investigate the influence of several Al laser ablation parameters on joint strength of laser welded Al – polyamide (PA6.6) assemblies. Significant parameters were highlighted, process window was outlined, and optimal parameters were identified. After assembly failure, the joint area was evaluated using optical microscopy. Depending on the laser ablation parameters, the joint area can be enhanced resulting in a significant increase in the corresponding bearable shear load.

© 2018 The Authors. Published by Elsevier Ltd. This is an open access article under the CC BY-NC-ND license

(<https://creativecommons.org/licenses/by-nc-nd/4.0/>)

Peer-review under responsibility of the Bayerisches Laserzentrum GmbH.

Keywords: Laser ablation; Laser beam welding; Hybrid joining; Metal-polymer assemblies

1. Introduction

Joining metals to polymers has gained cogent academic and industrial attention as these assemblies combines the thermal, mechanical, and electrical properties of the metals, with the low density and high deformability of polymers. Nowadays, such materials combination is mostly joined using mechanical or chemical methods. However, mechanical fasteners increases the assembly weight, and adhesive bonding escalates the manufacturing cost as it requires additional curing time. Contrarily, laser welding is a very promising rapid joining technique, particularly for its aptitude in creating miniaturized joints by precisely controlling the heat input to the weld joint.

Laser beam welding of metals, such as mild steel, stainless steel and aluminum to PA based polymers and fiber-reinforced composites, has already been demonstrated in literature [1]–[6]. Researchers [1]–[3] have been studying the effects of

mechanical and chemical surface pre-treatment techniques for metals on the joint strength. The use of a laser beam, as a tool for metallic surface pretreatment, has gained attention among researchers because of its appeal as a rapid, solventless and non-contact process, with considerably lower environmental impact compared to chemical pretreatments. Researchers have been studying the influence of patterned (cf. Figure 1.a) and stochastic surface structuring geometries (cf. Figure 1.c) on the joint strength.

Effects of forming uniformly distributed structures on Al and stainless steel surfaces, using Nd:YAG laser, before laser welding and thermal joining to selected polymers were examined [4]–[6]. The created structures allowed for mechanical interlocking, which was reported as one of the main causes behind the increase in joint strength. Holtkamp et al. [5] claimed a correlation between the increase in shear strength and laser surface structural density (per unit area).

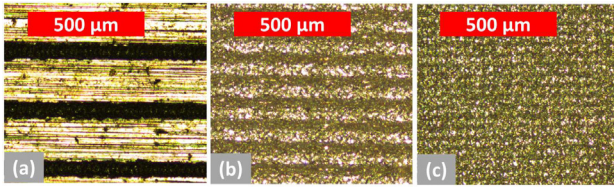


Figure 1. (a) patterned; (b) semi-patterned ;(c) stochastic ablation geometry.

Concerning stochastic surface structuring, researchers [7], [8] reported the effects of Al surface pretreatment, using short-pulsed laser ablation, prior to laser welding with PA6.6. However, the influence of the laser ablation parameters, on the joint strength and failure behavior, was not investigated.

2. Experimental method

This research considers patterned, semi-patterned, and stochastic laser surface pretreatment geometries (Figure 1). It highlights the most significant laser ablation processing parameters, defines the process window, and explores the failure behavior of laser welded Al – PA6.6 joints.

2.1. Materials

The materials used for these experiments were 0.5 mm thick EN-AW1050A aluminum, in half-hard state, and 4 mm polyamide 6.6 (PA6.6) purchased from Dutec. The Al sample had a geometry of 30 mm × 60 mm, while the PA6.6 sample had the dimensions of 25 mm × 75 mm. While the Al surface was prepared by laser treatment, PA samples was wiped with ethanol to remove potential dirt and grease from the surface prior to laser joining process.

2.2. Laser ablation DoE

Al surface was ablated by means of short-pulsed (ns) Nd:YVO4 laser (TruMark 6130 from TRUMPF) with a wave length of 1064 nm, and a spot size of 45 μm. The high power density caused the removal of surface contamination, and the formation of an aluminum oxidized layer at the surface [8].

Laser is introduced in the form of pulses on the Al surface. The pulses overlap ratio (o), shown in Figure 2 and described by Equation 1, is strongly influenced by three parameters: pulse frequency (f_p), beam deflection speed (V) and beam diameter (ϕ). Keeping a constant beam diameter and independently decreasing the pulse frequency or increasing the beam speed results in an increase in the overlap ratio. Thus, a combination of both parameters can produce patterned or stochastic surface structures. However, an increase in the pulse frequency causes a diminution in the peak pulse power (PPP).

First, Plackett-Burman [9] screening DoE was set, with the aid of Minitab software, to highlight the most significant parameters affecting the joint resistance to the applied shear load. Twenty-four experimental runs were designed to investigate seven parameters (Table 1). This design had a relatively high statistical power with 80% chance of detecting small effect size (shift in mean value) of 1.06 standard deviation. The joint strength was quantified by means of a single-lap shear test, using Z010 machine from Zwick/Roell.

$$o (\%) = \left(1 - \frac{V \left(\frac{mm}{s} \right)}{\phi (mm) \times f_p (Hz)} \right) \times 100 \quad (1)$$

Table 1: Screened variables.

Variables	Type	Low value	High value
Pulse frequency (kHz)	Continuous	15	40
Beam speed (mm/s)	Continuous	1776	3776
Lines	Categorical	Off	On
Focal position	Continuous	2.5mm offset	On surface
Rolling direction	Categorical	Axial	Perpendicular
Hatching orientation	Categorical	Axial	Perpendicular
Power percentage (%)	Continuous	50	75

For the screening design, two levels were chosen per variable. The beam deflection speed and pulse frequency were included in the design. Power percentage controls the peak pulse power (PPP) together with pulse frequency. 15 kHz yields an approximately calculated PPP of 85 kW, while 40 kHz yields 35 kW, as obtained from the machine manufacturer (TRUMPF). The focal position was varied from focusing on the Al surface with a spot size of 45 μm, to defocusing with a downward offset of 2.5 mm yielding a spot size of 102 μm.

Apart from continuous factors, the term “lines” refer to the laser scanning geometry. With this variable, the laser scans the geometry of a single line eight times with an offset equidistantly arranged in 4 mm wide geometry as shown in Figure 2. This causes the lines to overlap resulting in repetitive ablation of treated area. The term “rolling” corresponds to rolling grooves observed on raw Al. The term “hatch” corresponds to the alignment of the parallel laser beam structuring lines illustrated by the dashed lines in Figure 2. The distance between the hatching lines is influenced by the overlap ratio. Axial and perpendicular orientations are described with reference to the direction of the applied shear load.

Once important factors were identified, Response surface method (RSM) [10] was used in order to identify the factor settings that optimize the response. RSM is a statistical experimental design where the parameters are simultaneously varied in order to simulate their interaction. It also provides a predictive model relating the response to the process parameters. To outline the process window, four successive full-factorial experimental designs, with a total of 140 welded samples, were used to fit the model. Factors’ levels of the consecutive designs were determined by following the steepest path of ascent. Face-centered central composite design was used to model curvature. Analysis of Variance (ANOVA) [11] was employed to determine the reliability of the developed model and the significance of its coefficients.

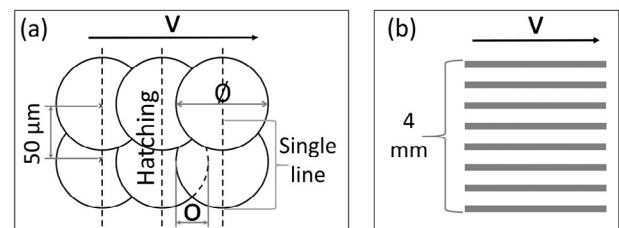


Figure 2. (a) schematic of overlapped pulses; (b) “lines” variable.

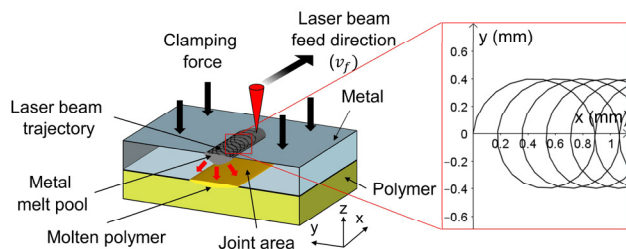


Figure 3. (left) Laser welding process schematic; (right) laser beam trajectory.

2.3. Laser beam welding

The laser welding was done using a fiber laser (TruFiber 400 from TRUMPF) with a wavelength of 1070 nm. The laser beam was irradiated on the Al surface, with a calculated spot diameter of 58 μm, after clamping the parts in an overlap configuration as shown in Figure 3. Part of the laser beam energy was absorbed, converted to heat energy, and conducted to the joint interface, thereby joining Al and PA6.6. Concerning the welding parameters, a peak pulse power of 400 W was modulated with a pulse frequency of 25 kHz, and a pulse duration of 35 μs. The laser beam followed a spiral trajectory with a corresponding feed velocity $v_f = 88.8$ mm/s (Figure 3). Those parameters gave joints with good resistance in previous studies [7], [8]. In order to investigate the sole effect of surface pre-treatment parameters, the laser welding parameters were kept fixed during the optimization and screening experiments.

2.4. Surface topography

Surface profile was obtained for all of the treated Al samples involved in the optimization experiments. The measurement was done according to ISO 4287 standard using TESA rugosurf 10G from TESA Technology. The measurement was aligned to the actual loading direction (axial to the shear load). The cut-off length was set to 0.8 mm with five cut-offs.

2.5. Macroscopic and microscopic assessments

After failure, microscopic and macroscopic images of the joint area were obtained using Leica DM4000 microscope, and a digital FUJIFILM X-Pro2 camera respectively. Five samples, ablated with different parameters, were assessed. The joint area was visually outlined and measured using GIMP software by counting the number of pixels and correlating with the pixel dimensions, which was determined using a reference scale included in the sample picture.

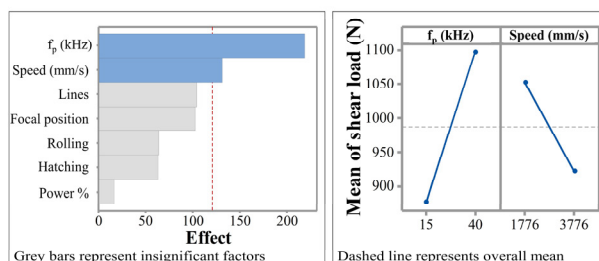


Figure 4. (left) Pareto chart of effects; (right) shear load main effect plot.

3. Results and discussions

3.1. Screening DoE

Screening design resulted in several ablation geometries, including patterned, semi-patterned, and stochastic (Figure 1). Pareto chart (Figure 4) shows the magnitude of effects of the screened parameters. Here, the effect of a single parameter illustrates the difference in mean shear load at its high and low values. The red line, determined by Lenth's method [12], shows the effect size at 0.1 level of significance. Results identified both pulse frequency and beam speed to have statistical significance on the achieved shear load.

The main effect plot, shown in Figure 4, describes how changes to a single factor affect the mean shear load. Results show that the high level of the pulse frequency and the low level of beam speed are favored to increase the shear load. This clearly manifests the benefit of increasing the overlap ratio. Thus, stochastic rather than patterned laser ablation geometry.

3.2. Optimization DoE

The critical factors, pulse frequency and beam speed, were used to create a predictive model. Insignificant variables were kept constant as shown in Table 2 during optimization.

Table 2: Fixed parameters settings during optimization DoE.

Power (%)	Focal position	Hatching	Lines	Rolling
100	On surface	Perpendicular	Off	Axial

Figure 5 shows the contour plot of the developed regression model (Equation 2). ANOVA analysis revealed the high reliability of the model and the significance of its coefficients, namely: pulse frequency (f_p [kHz]), beam speed (V [mm/s]), and non-linearity in speed (V^2). Such nonlinear behavior outlines an optimal range of overlap ratio between 60% and 75% as illustrated on the contour plot.

The maximum achievable pulse frequency of the laser ablation machine in use was 120 kHz. To further expand the process window, it was decided to lower the PPP by controlling the power percentage while keeping the overlap ratio ($\approx 68\%$) of the previously identified optimal setting (120 kHz and 1750 mm/s) unchanged. This last optimization step (Figure 5) revealed an optimal calculated PPP of ≈ 4.75 kW, achieving a maximum average shear load of 1465 ± 65 N.

$$Load (N) = 343.7 + 4.3 f_p + 0.68 V - 0.00019 V^2 \quad (2)$$

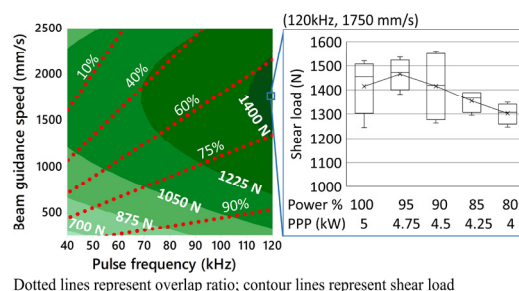


Figure 5. (left) contour plot of shear load; (right) expanding process window.

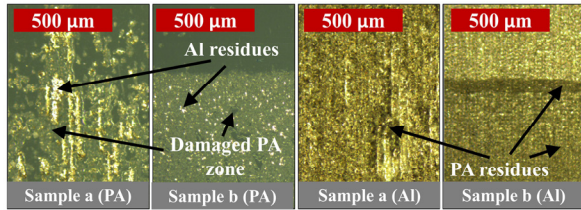


Figure 6. Welded region after fracture; (a) low (b) high shear load.

3.3. Surface topography

All ablated Al surfaces, excluding those ablated at 85 kHz and 250 mm/s (conditions “a”), showed comparable surface topography (average $R_a = 1 \pm 0.28 \mu\text{m}$). Samples ablated at conditions “a” (e.g. sample “a”, Figure 6) revealed a significantly higher R_a ($3.35 \pm 0.22 \mu\text{m}$) and failed at an average shear load of only $580 \pm 41 \text{ N}$.

3.4. Optical assessments after fracture

Microscopic images (Figure 6) reveals PA residues on fractured Al surface. The area of residual PA on Al side exhibited similar geometry to that of corresponding damaged area on the PA side. Traces of Al residues were also detected on the PA side. Therefore, it is assumed that failure is cohesive. Sample “a” exhibits a low value, and inhomogeneous geometrical distribution, of joint area compared to “b”. This can be explained by the increase in thermal contact resistance at the interface, as a result of increased Al surface roughness [13]. Further characterization of the surfaces after fracture and discussion of its link with failure mode and shear strength of the assembly are beyond the scope of this study.

The area of residues/damages on both materials after failure is quantified and assumed to present the joint area. Figure 7 shows a linear relation between the weld joint area, of five differently ablated samples, and their corresponding shear load. A descriptive regression model was generated to describe the relation between all data points. High coefficient of determination (R^2) value (0.96) indicates that this linear relation describes 96% of the variation in response, and features negligible variations in calculated strength. Interestingly, this linear relation highlights a constant shear stress among all tested samples regardless of the laser ablation parameters. The slope of the descriptive regression model denotes a shear stress of 35.44 MPa. Results confirms that laser ablation parameters have a strong influence on the joint area and quality, but no impact on the joint stress at failure.

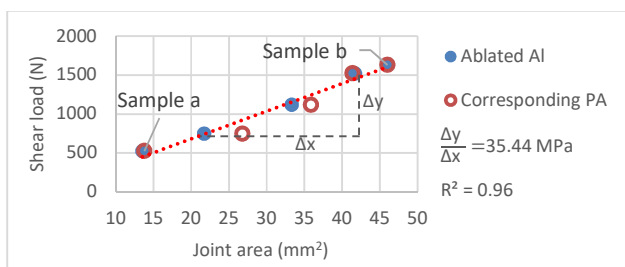


Figure 7. Relation between shear load and joint area.

4. Conclusion

A design of experiments was developed to investigate the influence of short-pulsed laser ablation parameters to treat Al surface before laser welding to PA6.6. Screening results highlighted the significance of pulse frequency and beam guidance speed on the joint resistance to the applied shear load, with preferences to stochastic structuring geometry. A developed regression model shows a directly proportional linear relation between the shear load and the pulse frequency, and a nonlinear relation with the beam guidance speed. Optimal laser ablation parameters were identified at a spot size of 45 μm , along with a peak pulse power of $\approx 4.75 \text{ kW}$ and an overlap ratio of $\approx 68\%$, which are calculated at pulse frequency of 120 kHz and beam speed of 1750 mm/s.

Joint area was evaluated optically after failure. Results showed that joint area is linearly correlated to joint shear load. This leads to the conclusion that laser ablation parameters have a strong influence on the joint quality, through the value of joint area, but no influence on the joint stress at failure.

Acknowledgments

The authors would like to acknowledge FNR (Luxembourg), and DGO6 (Wallon region, Belgium) for their financial support in this research work through the LaserSTAMP project.

References

- [1] J. P. Bergmann and M. Stambke, “Potential of laser-manufactured polymer-metal hybrid joints,” *Phys. Procedia*, vol. 39, pp. 84–91, 2012.
- [2] Z. Zhang, J. G. Shan, X. H. Tan, and J. Zhang, “Effect of anodizing pretreatment on laser joining CFRP to aluminum alloy A6061,” *Int. J. Adhes. Adhes.*, vol. 70, pp. 142–151, 2016.
- [3] A. Klotzbach, M. Langer, R. Pautzsch, J. Standfuß, and E. Beyer, “Thermal direct joining of metal to fiber reinforced thermoplastic components,” vol. 022421, no. 806, 2017.
- [4] P. Amend, S. Pfindel, and M. Schmidt, “Thermal joining of thermoplastic metal hybrids by means of mono- and polychromatic radiation,” *Phys. Procedia*, vol. 41, pp. 98–105, 2013.
- [5] J. Holtkamp, A. Roesner, and A. Gillner, “Advances in hybrid laser joining,” *Int. J. Adv. Manuf. Technol.*, vol. 47, no. 9–12, pp. 923–930, 2010.
- [6] A. Roesner, S. Scheik, A. Olowinsky, A. Gillner, U. Reigen, and M. Schleser, “Laser assisted joining of plastic metal hybrids,” *Phys. Procedia*, vol. 12, no. PART 2, pp. 373–380, 2011.
- [7] C. Lamberti, T. Solchenbach, P. Plapper, and W. Possart, “Laser Assisted Joining of Hybrid Polyamide-Aluminum Structures,” *Phys. Procedia*, vol. 56, no. 8, pp. 845–853, 2014.
- [8] A. Al-Sayyad et al., “Influence of laser ablation and plasma surface treatment on the joint strength of laser welded aluminum-polyamide assemblies,” in *JNPLI 2017*, 2017.
- [9] R. L. PLACKETT and J. P. BURMAN, “THE DESIGN OF OPTIMUM MULTIFACTORIAL EXPERIMENTS,” *Biometrika*, vol. 33, no. 4, pp. 305–325, 1946.
- [10] G. E. P. Box and K. B. Wilson, “On the experimental attainment of optimum conditions,” in *Breakthroughs in statistics*, Springer, 1992, pp. 270–310.
- [11] R. H. Myers, D. C. Montgomery, and C. M. Anderson-cook, *Response Surface Methodology*. 2009.
- [12] R. V. Lenth, “Quick and Easy Analysis of Factorials Unreplicated,” *Technometrics*, vol. 31, no. 4, pp. 469–473, 1989.
- [13] C. V. Madhusudana, *Thermal contact conductance*, 2nd ed. Springer, 2014.

